THE JOURNAL OF BIOLOGICAL CHEMISTRY VOL. 290, NO. 21, pp. 13157–13167, May 22, 2015

Expression of Ceramide Synthase 6 Transcriptionally Activates Acid Ceramidase in a c-Jun N-terminal Kinase (JNK)-dependent Manner*

Received for publication, December 9, 2014, and in revised form, March 3, 2015 Published, JBC Papers in Press, April 3, 2015, DOI 10.1074/jbc.M114.631325

Tejas S. Tirodkar[‡], Ping Lu[‡], Aiping Bai[§], Matthew J. Scheffel[‡], Salih Gencer[§¶], Elizabeth Garrett-Mayer[‖], Alicja Bielawska[§], Besim Ogretmen[§1], and Christina Voelkel-Johnson[‡2]

From the Departments of [‡]Microbiology and Immunology, [§]Biochemistry and Molecular Biology, and [‖]Public Health, Medical University of South Carolina, Charleston South Carolina 29425 and the [¶]Department of Molecular Biology and Genetics, 34662 Istanbul, Turkey

Background: Ceramide is important for cellular signaling.
Results: Increasing the expression of ceramide synthase 6 (CerS6) results in transcriptional activation of acid ceramidase independent of catalytic CerS6 activity.
Conclusion: Modulation of a single member of the ceramide synthase family impacts on sphingolipid composition and ceramide metabolizing enzymes.
Significance: Understanding how CerS impacts gene expression and signaling is important for the development of novel therapeutic approaches.

A family of six ceramide synthases with distinct but overlapping substrate specificities is responsible for generation of ceramides with acyl chains ranging from ~14–26 carbons. Ceramide synthase 6 (CerS6) preferentially generates C_{14}- and C_{16}-ceramides, and we have previously shown that down-regulation of this enzyme decreases apoptotic susceptibility. In this study, we further evaluated how increased CerS6 expression impacts sphingolipid composition and metabolism. Overexpression of CerS6 in HT29 colon cancer cells resulted in increased apoptotic susceptibility and preferential generation of C_{16}-ceramide, which occurred at the expense of very long chain, saturated ceramides. These changes were also reflected in sphingomyelin composition. HT-CerS6 cells had increased intracellular levels of sphingosine, which is generated by ceramidases upon hydrolysis of ceramide. qRT-PCR analysis revealed that only expression of acid ceramidase (ASAH1) was increased. The increase in acid ceramidase was confirmed by expression and activity analyses. Pharmacological inhibition of JNK (SP600125) or curcumin reduced transcriptional up-regulation of acid ceramidase. Using an acid ceramidase promoter driven luciferase reporter plasmid, we demonstrated that CerS1 has no effect on transcriptional activation of acid ceramidase and that CerS2 slightly but significantly decreased the luciferase signal. Similar to CerS6, overexpression of CerS3–5 resulted in an ~2-fold increase in luciferase reporter gene activity. Exogenous ceramide failed to induce reporter activity, while a CerS inhibitor and a catalytically inactive mutant of CerS6 failed to reduce it. Taken together, these results suggest that increased expression of CerS6 can mediate transcriptional activation of acid ceramidase in a JNK-dependent manner that is independent of CerS6 activity.

Sphingolipids are important signaling molecules and can significantly impact on cellular function. Ceramide, the central molecule in sphingolipid biosynthesis, can be generated through the action of ceramide synthases (CerS)[3] in the *de novo* or the salvage pathway (1). CerS comprise a family of six enzymes that preferentially conjugate a fatty acyl-CoA moiety to the sphingoid base, thereby generating ceramides with fatty acid side chains ranging from 14 to 26 carbons. Recent studies have demonstrated associations between specific ceramide species and cellular responses (2).

We have previously shown that RNAi-mediated down-regulation of CerS6 results in a specific decrease in C_{16}-ceramide and increased resistance to the death receptor ligand TRAIL whereas overexpression of CerS6 increased susceptibility to TRAIL (3). CerS6 has also been implicated to contribute to apoptosis induced by 17AAG (4) and MDA-7 (5), the combination of sorafenib and vorinostat (6, 7), celecoxib-mediated chemoprevention of colon cancer (8), and efficacy of photodynamic therapy (9). These studies suggest that CerS6 activity contributes to the efficacy of existing therapies and might be a potential biomarker to predict responsiveness.

Evidence that CerS can have opposing and tissue-specific roles is also emerging. Thus while several studies have found links between CerS6/C_{16}-ceramide and apoptosis (10), overexpression of CerS2, which generates C_{24}-ceramides can promote proliferation and offer protection against radiation-induced cell death (11, 12). Generation of CerS-deficient mice is revealing tissue-specific effects as well. For example, knock out of

* This project was supported by MUSC intramural funds (to C. V. J.) and in part by the Lipidomics and Flow Cytometry Shared Resources, Hollings Cancer Center, MUSC (P30 CA138313).
[1] Supported by CA88032, CA173687, and DE016572.
[2] Supported by National Institutes of Health Grant P01 CA154778. To whom correspondence should be addressed: Dept. of Microbiology and Immunology, Medical University of South Carolina, 173 Ashley Ave., Charleston, SC. Tel.: 843-792-3125; Fax: 843-792-9588; E-mail: johnsocv@musc.edu.

[3] The abbreviations used are: CerS, ceramide synthase; JNK, Jun N-terminal kinase; SM, sphingomyelin; AdCerS6, adenovirus-expressing CerS6.

CerS2, which is expressed at similar levels in the mouse liver and kidney, results in liver abnormalities while kidney function remains normal (13, 14). CerS6 also appears to have tissue-specific effects as decreased expression induces ER stress and apoptosis in head and neck squamous carcinoma cells but not in A549, MCF-7, or SW480 cells, which were derived from lung, breast, and colon cancer, respectively (3, 15, 16).

Altered ceramide distributions and/or changes in ceramide synthase expression are beginning to be associated with specific diseases (17). For example, elevated expression of CerS6 has recently been suggested to play a role in the onset of disease in chronic experimental autoimmune encephalomyelitis, a model of multiple sclerosis (18). CerS6 is highly expressed in the intestinal tract (19), and we have therefore focused our investigations on the role of CerS6 in colon cancer. In HCT-116 colon cancer cells overexpression of CerS6 induced spontaneous apoptosis (11). In our hands elevated expression of CerS6 in SW620 colon cancer cells did not result in spontaneous apoptosis but increased susceptibility to apoptotic stimuli (3). However, the consequence of CerS6 expression was not previously investigated in detail, and we hypothesized that due to the highly dynamic nature of sphingolipid metabolism (13, 14, 20, 21), alterations in the expression of CerS6 may have impacts beyond increased generation of C_{16}-ceramide. In support of this hypothesis, the current study reveals a novel connection between ceramide synthases and acid ceramidase.

Experimental Procedures

Cell Culture—The cell lines HT29, SW480, SW620, and HEK293A were purchased from ATCC (Manassas, VA) and maintained in DMEM medium (MediaTech, Manassas, VA) supplemented with 10% heat-inactivated FBS (Hyclone, Logan, UT), 1% Antibiotic-Antimycotic (MediaTech), and 0.1% Gentamycin (Lonza BioWhittaker, Walkersville, MD) and cultured at 37 °C, 5% CO_2 in humidified air.

Plasmids and Adenovirus—pCerS6-IRES-GFP has previously been described (3). Additional CerS plasmids were generated by removing the transgene cassette from pCMV-Tag2B (kindly provided by Dr. Futerman (Weizmann Institute of Science, Rehovot, Israel) (22) using BamHI and SalI (for CerS1, 4, 6) or NheI and SalI (for CerS2, 3, 5) and inserting them into the BglII/SalI or NheI/SalI sites in pIRES2-EGFP (Clontech, Mountain View, CA) respectively. pIRES2-EGFP served as the control plasmid in all experiments. The pGL3-ASAH1 reporter plasmid (containing the entire ASAH1 promoter region from −2740 to +1) was generously provided by Dr. Marion Sewer (UCSD, San Diego, CA) (23), and plasmids expressing wild type and mutant CerS6 (H212A) were obtained from Dr. Besim Ogretmen (15). The shRNA against CerS6 was inserted into pLKO-Tet-On (AddGene), which is a single vector inducible shRNA system (24). Oligos were ordered from IDT (5′-CCGGGAACTGCTTCTGGTCTTACTT*ACGCGT*AAAGTAAGACCAGAAGCAGTTCTTTTT-3′ and 5′-AATTAAAAAGAACTGCTTCTGGTCTTACTTT*ACGCGT*AAGTAAGACCAGAAGCAGTTC-3′), annealed and ligated into AgeI/EcoRI sites pLKO-tet-On. An internal MluI site (shown in italics) in the oligo was used to screen clones for inserted DNA, which was then verified by sequencing.

The adenovirus expressing CerS6 was generated using the AdEasy system (ATCC) (25). Briefly, the EcoRI and HindIII fragment from pCerS6-IRES-GFP was subcloned into the Shuttle vector, which was then recombined with the AdEasy vector in the *Escherichia coli* BJ5183 strain. Following screening by PacI digestion, DNA of positive recombinants was transiently transfected into HEK293A cells using Lipofectamine 2000 and CerS6 expression verified by Western blot. A positive recombinant was transfected into HEK293A cells, and cultures were observed for formation of viral plaques (25). Crude viral lysate was provided to Vector Biolabs (Philadelphia, PA, for amplification and determination of titer). The control adenovirus was also obtained from Vector Biolabs.

Flow Cytometry—Flow cytometry (LSRFortessa) and cell sorting (MoFlo) was performed in the MUSC flow cytometry shared resource.

Transfections and Transductions—HT29 transfectants expressing CerS6 or GFP only were generated by transfection of pCerS6-IRES-GFP (3) or pIRES-GFP plasmids using Lipofectamine 2000 (Invitrogen, Grand Island, NY) followed by selection and maintenance in 1.5 mg/ml neomycin (Fisher Scientific). Experiments with stably transfected mass clones were performed within 25 passages. HT29 cells expressing pGL3-ASAH1 were generated by co-transfection with a G418 resistance plasmid and selected as above. SW480 were transfected with pLKO-Tet-On shRNA-CerS6 followed by selection in 1 μg/ml puromycin.

For adenoviral transductions, cells were plated overnight and the next day adenovirus added to the culture medium at the indicated concentration. Luciferase activity was measured 4 days post-infection.

Transient transfections of HEK293A cells were performed in 96-well plates using 200 ng DNA and 0.5 μl Lipofectamine per well according to the manufacturer's instructions.

Chemicals—Curcumin and SP600125 were purchased from Alexis and Calbiochem, respectively. LCL-23 (C_6-ceramide), LCL-24 (C_{16}-ceramide), and LCL-521 (26) were obtained from the MUSC Lipidomics facility. Fumonison B1 was purchased from Acros Organics.

Viability and Luciferase Activity Assays—Viability was measured using the CellTiterBlue substrate and luciferase activity was determined using the Steady-Glo kit. Both kits were purchased from Promega (Madison, WI). Signals were quantified using a BMG Optima plate reader.

Real-time PCR—Cells were plated on 100 mm dishes and allowed to form a monolayer for 2 days. Pellets from 5 million cells were lysed, processed over QIAShredder columns, and RNA isolated using an RNeasy kit (Qiagen, Valencia, CA). Following DNase (Qiagen) treatment, 3 μg of RNA was used to prepare cDNA using the Stratagene AffinityScript QPCR cDNA synthesis kit (Stratagene, Santa Clara, CA) in a 20 μl reaction. The cDNA was diluted 1:8, and 2 μl used as template for each qPCR reaction. The qPCR reaction contained 0.2 μM 1:1 Forward and Reverse primers and iQ SYBR Green Supermix (Bio-Rad) as directed by the manufacturer. Primers against human CerS6 (Hs00826756) were purchased from Applied Biosystems (Carlsbad, CA) and GAPDH primers (VHPS-3541) were obtained from Realtimeprimers.com (Elkins Park, PA).

Custom primers were synthesized by IDT (Coralville, IA) using the following sequences: endogenous CerS6-Forward: 5′-ACATTCCTTCAGCCTCCTGGAGTT-3′, Reverse: 5′-GCTCCCTGGTTTCCAGGCCAC-3′; ASAH1-Forward: 5′-TCTTCCTTGATGATCGCAGAACGCC-3′; Reverse: 5′-ACGGTCAGCTTGTTGAGGAC-3′. The reaction was performed on a Bio-Rad CFX-96 cycler. Expression levels were calculated using the 2^(−ΔΔ) computation and expressed relative to GAPDH.

Sphingolipid Analysis and Metabolic Labeling—Sphingolipid analysis was performed as described previously (27). The cell pellets were stored at −80 °C until processing for sphingolipid analysis by liquid chromatography/mass spectrometry (LC-MS/MS) in the MUSC Lipidomics facility (28). An aliquot of the lipid extract was used to carry out lipid phosphate estimation using Bligh Dyer extraction and a colorimetric assay (29). For sphingolipid metabolic labeling, cells were incubated with 1 μM ^{17}C-sphingosine (Avanti Polar Lipids) for 30 min. The LC-MS/MS analysis was modified to detect only ^{17}C-sphingolipids (30).

Western Blot Analysis—Western blot analysis was performed as previously described (27). Following electrophoresis and transfer of proteins, nitrocellulose membranes were probed with antibodies against ceramide synthase 6 (1:1000, Abnova or Abcam), acid ceramidase (1:1000, BD Pharmingen), PARP (1:1000, Cell Signaling Technology), c-jun (Ser63) (1:500, Cell Signaling Technology), and/or actin (1:2000, Sigma). HRP-labeled secondary anti-mouse or anti-rabbit antibodies were purchased from Santa Cruz Biotechnology. Signal was detected using the WestDura chemiluminescence substrate (Thermo Scientific).

In Vitro Acid Ceramidase Activity Assay—Cells were plated at a density of 1×10^7 cells on 150-mm dishes and allowed to form a monolayer for 2 days. At harvest, cells were counted and lysed in an acidic buffer (50 mM sodium acetate, 5 mM magnesium chloride, 1 mM EDTA, and 0.5% Triton X-100, pH 4.5) to determine acid ceramidase activity as previously (26). The assay was carried out in duplicate using an equal amount of protein lysate (close to 200 μg), and results displayed as pmol palmitate liberated per hour per mg protein.

Statistical Analysis—Differences in viability and lipid composition were determined in the unpaired Student's *t* test using the GraphPad software. To evaluate differences in fold-change of luciferase activity in transient transfections experiment in HEK293A cells, we used a hierarchical linear mixed effects regression model that was fit with the main effects of marker (CerS1, CerS2, etc.) and nested random effects for experiment and well over 10 cycles (10 min/cycle) of luciferase activity. Regression coefficients and their standard errors were used for making inferences regarding statistical significance at the $\alpha = 0.05$ level. Fold-change and S.E. were based on model results.

Results

Cells with Elevated CerS6 Expression Have Increased Susceptibility to TRAIL and 5-Fluorouracil Chemotherapy—HT29 colon carcinoma cells were stably transfected with pCerS6-IRES2-EGFP or pIRES2-GFP plasmids to generate HT-CerS6 and HT-GFP cells, respectively. Analysis of mRNA from G418-resistant mass clones indicated that total CerS6 transcript levels increased ~3-fold in the HT-CerS6 transfectants compared with the HT-GFP cells (Fig. 1*A*). Levels of endogenous CerS6 mRNA were not significantly changed (Fig. 1*A*). These results

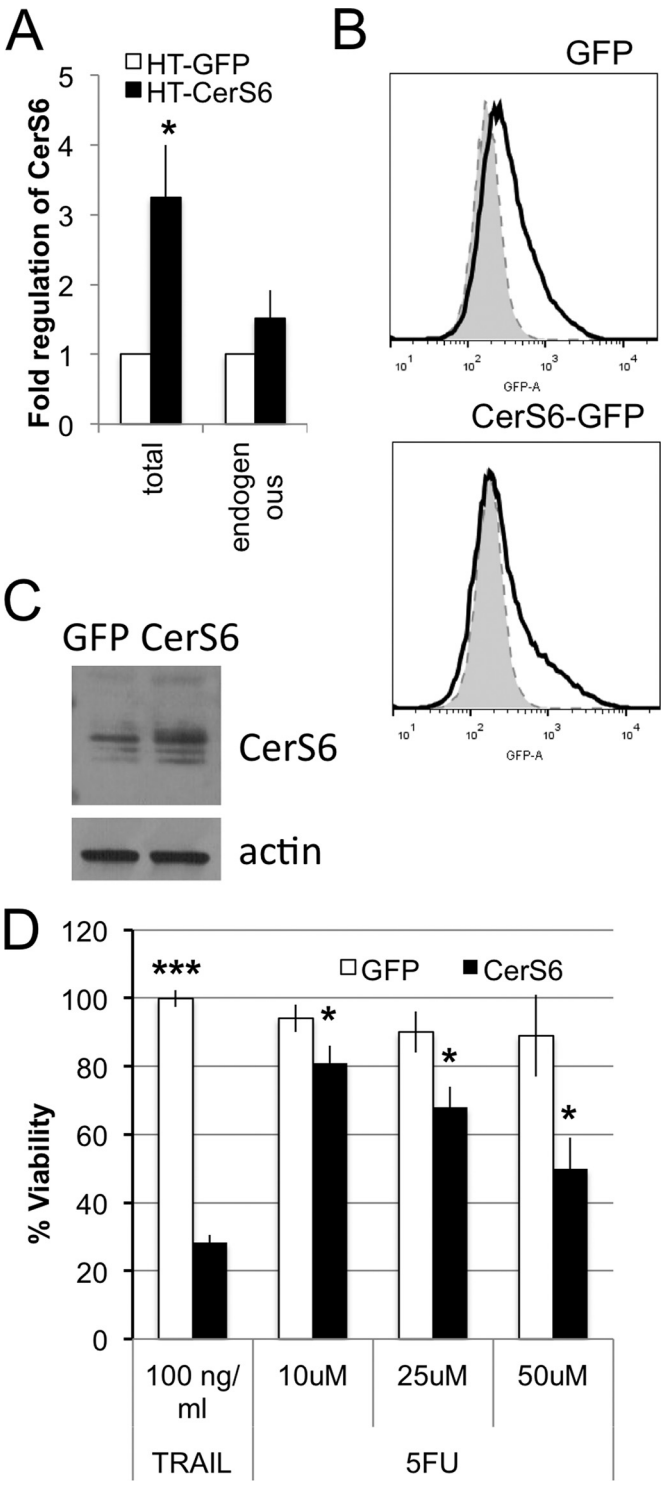

FIGURE 1. **CerS6 expression and susceptibility.** *A*, qRT-PCR analysis of total CerS6 and endogenous CerS6 mRNA. Data are from 3 separate mRNA isolations. *B*, GFP detection within mass clones by flow cytometry. *C*, Western blot analysis of CerS6 expression in HT29 cells transfected with GFP or CerS6. Analysis was performed on populations sorted for GFP expression. Actin serves as a loading control. *D*, HT-GFP and HT-CerS6 cells were treated with 100 ng/ml TRAIL for 24 h or 5-fluorouracil for 72 h. Data are the mean ± S.E. from three separate experiments. *, $p < 0.05$; ***, $p < 0.0005$.

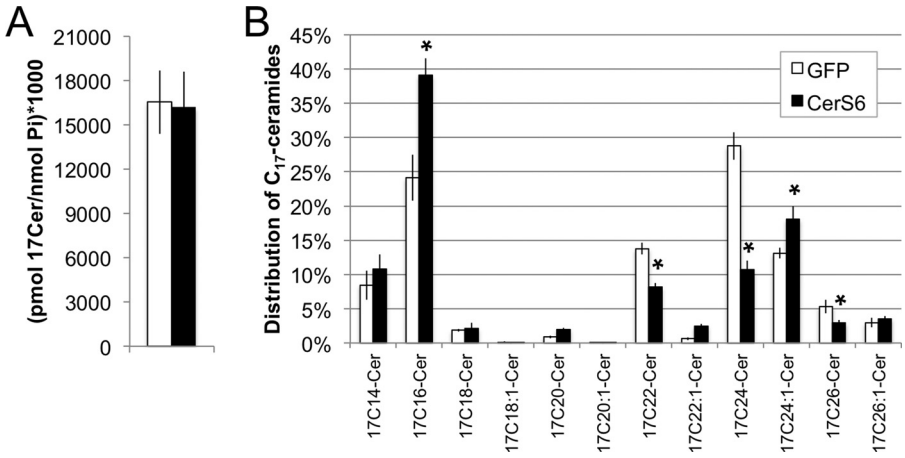

FIGURE 2. **Metabolic labeling of ceramides.** *A*, generation of total ^{17}C-labeled ceramides normalized to lipid phosphate. *B*, distribution of ^{17}C-labeled ceramides by species. Data shown are the mean ± S.E. from three independent experiments. *, $p < 0.05$.

suggest that the increase in total CerS6 mRNA resulted from expression of the transgene. Based on GFP expression, at least 20% of cells within mass clones expressed the transgene (Fig. 1*B*). An increase in CerS6 protein in the mass clone was observed when GFP-positive cells were analyzed by Western blot following sorting by flow cytometry (Fig. 1*C*). Consistent with our previous findings in SW620 cells, elevating CerS6 increased susceptibility of HT29 cells to the death ligand TRAIL (Fig. 1*D*). Sensitivity to 5-fluorouracil, a chemotherapeutic agent frequently used in colorectal patients, was also enhanced in HT-CerS6 cells compared with HT-GFP (Fig. 1*D*).

Up-regulation of CerS6 Expression Increases C_{16}-ceramide Generation at the Expense of Very Long Chain Ceramides—Although cells expressing elevated CerS6 are more susceptible to cell death, the exact impact of CerS6 expression on sphingolipids in stably transfected cells has not previously been determined. Therefore, we next used a cell-based assay, in which ^{17}C-sphingosine serves as a metabolic label, to determine how increased expression of CerS6 impacts on the incorporation of sphingosine into ceramides. HT-GFP and HT-CerS6 cells were incubated with 1 μM ^{17}C-sphingosine for 30 min followed by analysis of the ^{17}C-sphingolipid profile. Total ^{17}C-ceramide levels were similar between the GFP and the CerS6 transfectants (Fig. 2*A*), indicating that the total cumulative activity of CerS, at least in the salvage pathway in which sphingosine is recycled into ceramides, is comparable between HT-GFP and HT-CerS6 cells. The majority of ^{17}C-sphingosine was incorporated into $^{17}C_{16}$-, $^{17}C_{22}$-, and $^{17}C_{24}$-ceramides (Fig. 2*B*) but CerS6 expression influenced the distribution of ceramide species. Compared with HT-GFP, HT-CerS6 cells contained significantly more $^{17}C_{16}$- and $^{17}C_{24:1}$-ceramides and significantly less $^{17}C_{22:0}$-, $^{17}C_{24:0}$, and $^{17}C_{26:0}$-ceramides. These results suggest that increased generation of C_{16}-ceramide occurs at the expense of very long chain (C_{22}-C_{26}) saturated but not unsaturated ceramides.

Changes in ceramide composition observed in the metabolic labeling assay were also reflected at the steady state, *i.e.* the very long chain saturated ceramides $C_{24:0}$-ceramide and $C_{26:0}$-ceramide were significantly decreased while C_{16}-ceramide and $C_{24:1}$-ceramide were increased (Fig. 3*A*). Similar results were observed in SW620 cells upon adenoviral expression of the CerS6 transgene (data not shown), which suggests that CerS6-mediated alterations in ceramide species distribution is not cell

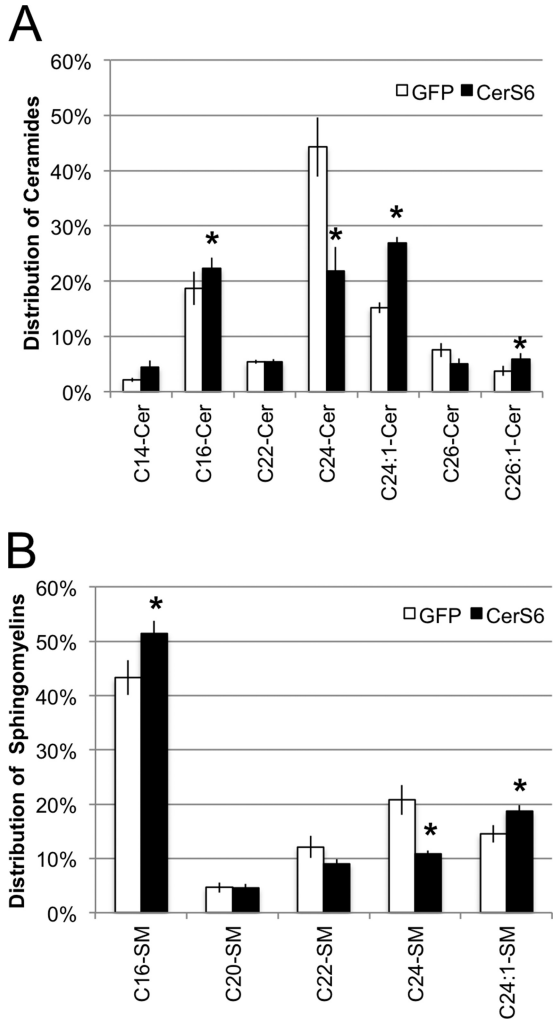

FIGURE 3. **Steady state sphingolipid composition of HT-GFP and HT-CerS6 cells.** Distribution of ceramides (*A*) and sphingomyelin (*B*). Only species that represent at least 3% of the total pool of ceramide or sphingomyelin were included. Data shown are the mean ± S.E. from three independent experiments. *, $p < 0.05$.

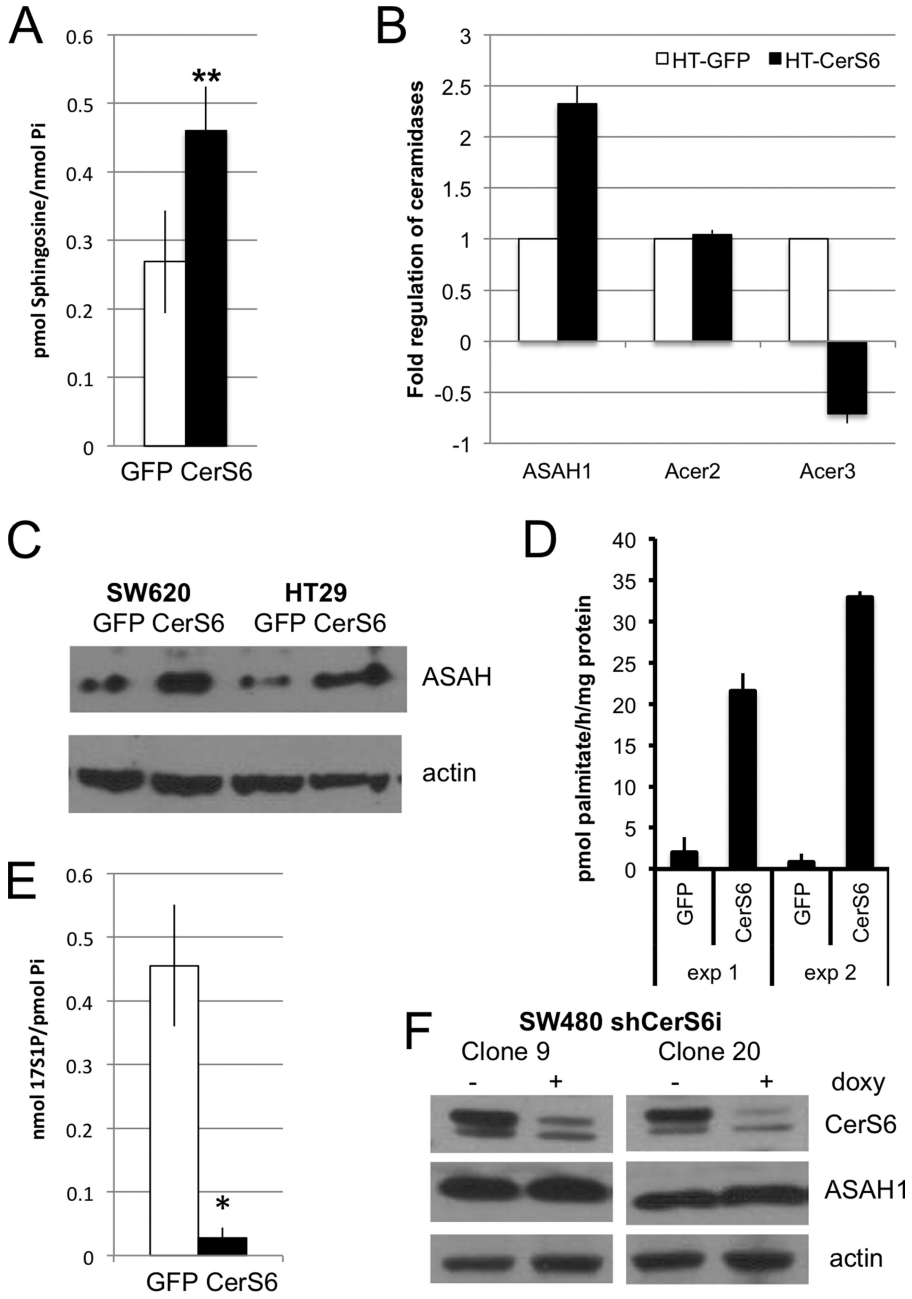

FIGURE 4. **Analysis of sphingosine and ceramidases.** *A*, steady state intracellular levels of sphingosine in HT-GFP and HT-CerS6 cells normalized to inorganic phosphate. Data shown are the mean ± S.E. from three independent experiments. **, $p < 0.005$. *B*, qRT-PCR analysis of ceramidase mRNA. Data shown are from at least two independent determinations. *C*, Western blot analysis of acid ceramidase in SW620 and HT29 cells stably transfected with GFP or CerS6. Actin serves as loading control. *D*, acid ceramidase activity assay. Each assay was performed in triplicate. *E*, incorporation of ^{17}C-sphingosine into sphingosine-1-phosphate. Data shown are the mean ± S.E. from two independent experiments. *F*, Western blot analysis of two individual clones of SW480 cells stably transfected with an inducible shRNA that targets CerS6. Protein lysates, generated after induction of shRNA expression for 1 week, were analyzed for CerS6 and acid ceramidase expression. Actin serves as loading control.

line specific. Since ceramide can be further metabolized into complex sphingolipids, sphingomyelin (SM) composition was also analyzed. We found that expression of CerS6 increased the C_{16}-SM content from 43% in HT-GFP cells to 51% in HT-CerS6 cells (Fig. 3*B*). This significant increase in C_{16}-SM was accompanied by an almost 50% decrease in $C_{24:0}$-SM. The increase in $C_{24:1}$-Cer in HT-CerS6 cells corresponded to an increase in $C_{24:1}$-SM (Fig. 3*B*). These results suggest that changes in ceramide composition as a consequence of increased CerS6 expression are also reflected in complex sphingolipids such as sphingomyelin.

HT-CerS6 Cells Have Elevated Acid Ceramidase Expression and Activity—In addition to being incorporated into complex sphingolipids, ceramide can also be hydrolyzed to sphingosine by ceramidases. We found that HT-CerS6 cells contained nearly twice as much sphingosine as HT-GFP cells (Fig. 4*A*). Five ceramidases, including ASAH1, ASAH2, and ACER1–3, have been identified. The gene threshold for ASAH2 and

ACER1 was high (>30) indicating that the relative expression levels of these genes are low in HT29 cells. Of the remaining ceramidases, mRNA levels were increased only for acid ceramidase (ASAH1) (Fig. 4*B*). Western blot analysis of two colon cancer cells confirmed that ASAH1 expression is elevated when CerS6 is overexpressed (Fig. 4*C*). An *in vitro* assay confirmed that acid ceramidase activity is also higher in HT-CerS6 cells than in HT-GFP cells (Fig. 4*D*).

Sphingosine serves not only as substrate for ceramide synthases in the salvage pathway but can also be further metabolized to sphingosine-1-phosphate (S1P) through the action of sphingosine kinases. Steady state levels of intracellular S1P were below detection in our analysis. We therefore used ^{17}C-sphingosine as the substrate for metabolic labeling and found that HT-CerS6 had a significantly reduced capacity to generate S1P compared with HT-GFP cells (Fig. 4*E*).

Our results suggested that increasing CerS6 results in elevated expression of acid ceramidase. To investigate if decreasing CerS6 reduces acid ceramidase expression we chose SW480 cells, which express higher levels of CerS6 than the isogenic SW620 cells used in overexpression studies (3). SW480 cells were transfected with an inducible shRNA against CerS6 and analysis for acid ceramidase performed in two individual clones. As shown in Fig. 4*F*, knockdown of CerS6 did not appear to decrease acid ceramidase expression.

Increased Expression of Acid Ceramidase in Response to CerS6 Expression Occurs via a JNK-AP1-dependent Mechanism and Is Important for Survival—We hypothesized that increased expression and activity of acid ceramidase occurs in response to increased generation of C_{16}-ceramide. Ceramide stress has been shown to activate the JNK pathway (31–33) and more recently it has been shown that radiation-induced ceramide stress and subsequent up-regulation of acid ceramidase occurs in an AP-1-dependent manner (34). Therefore, we treated HT-CerS6 cells with the JNK inhibitor SP600125 or curcumin, a natural compound with anti-tumor activity that has been shown to directly interfere with DNA binding at the AP-1 transcription factor (35, 36), and examined the impact on phosphorylation of c-jun and acid ceramidase expression. Compared with HT-GFP cells, HT-CerS6 cells had increased phosphorylation of c-jun on Ser-63 (Fig. 5*A*). Treatment with the JNK inhibitor SP600125 decreased phosphorylation of c-jun to undetectable levels. In contrast to SP600125, curcumin did not decrease phosphorylation of c-jun, which is consistent with its function of inhibiting AP-1 DNA binding downstream of c-jun. Treatments with either SP600125 or curcumin also diminished levels of acid ceramidase (Fig. 5*A*). Morphological assessment of treated cultures suggested that HT-CerS6 cells were beginning to die when exposed to inhibitors of the JNK pathway. Analysis of PARP, a marker of apoptosis, confirmed that this protein was cleaved when HT-CerS6 cells were treated with SP600125 or curcumin.

To more directly quantify the effect of SP600125 and curcumin on viability, HT-GFP and HT-CerS6 cells were cultured in the absence or presence of these agents. As shown in Fig. 5*B*, HT-CerS6 cells were significantly more susceptible to SP600125 than control cells. Viability in the presence of curcumin was also reduced but did not reach statistical significance.

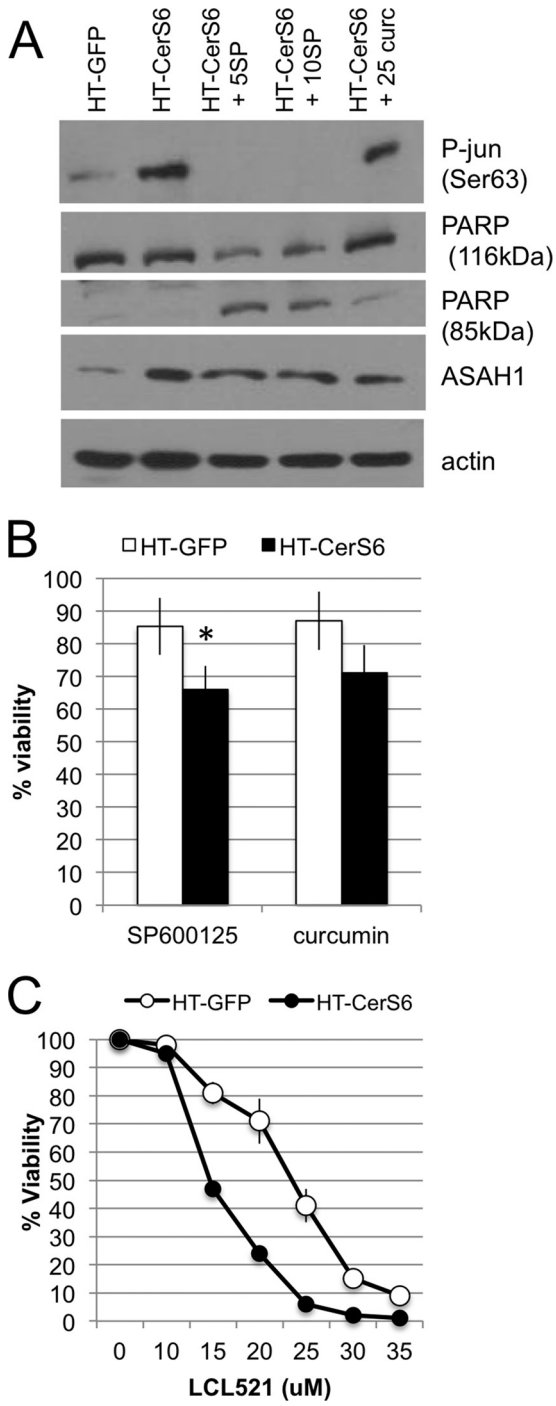

FIGURE 5. **The impact of pharmacological inhibitors or protein expression and viability in HT-GFP and HT-CerS6 cells.** *A*, Western blot analysis of cells treated with 5 or 10 μM SP600125 and 25 μM curcumin for 28 h. *B*, viability in the presence of SP600125 or curcumin was measured over 3 days and results expressed as a percentage of untreated cells. Data shown are the average ± S.D. from three experiments. *C*, cell viability in the presence of LCL-521 after 24 h of treatment. A representative experiment performed in triplicate is shown. Similar results were obtained in two additional analyses.

Taken together, the results suggested that inhibition of acid ceramidase expression by either SP600125 or curcumin may be responsible for induction of PARP cleavage and preferentially decreased viability of HT-CerS6 cells. To directly test how inhibition of acid ceramidase impacts on viability, HT-GFP and HT-CerS6 cells were treated with the acid ceramidase inhibitor

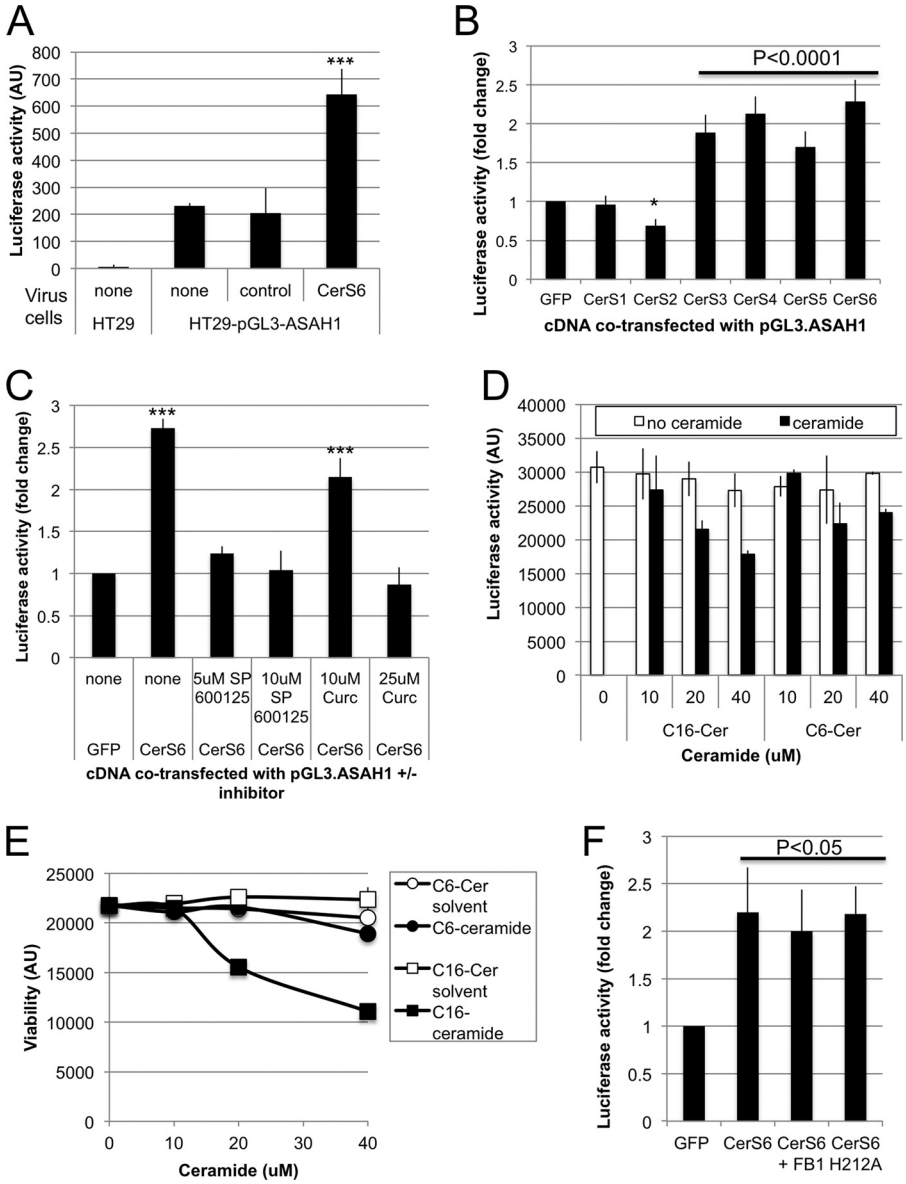

FIGURE 6. **Transcriptional activation of acid ceramidase.** *A*, HT29 -pGL3-ASAH1 cells were infected with 300 MOI of control or AdCerS6 and luciferase activity determined 4 days post-infection. A representative experiment performed in duplicate is shown. *B*, HEK293A cells were transiently co-transfected with pGL3-ASAH1 and various plasmids expressing CerS. Luciferase activity was determined 28 h post-transfection. Results shown are the mean fold-increase ± S.E. from four independent experiments. *C*, HEK293A cells were transiently co-transfected with pGL3-ASAH1 and pCerS6-IRES-GFP in the absence and presence of pharmacological inhibitors. Luciferase activity was determined 28 h post-transfection. Results shown are the mean fold-increase ± S.E. from two independent experiments. *D*, HEK293A cells were transiently transfected with pGL3-ASAH1 and exogenous ceramide (or solvent control) was added 22 h post-transfection for an additional 6 h. The solvent control for C_6- and C_{16}-ceramide were methanol and methanol:dodecane (1:1), respectively. Luciferase activity was determined 28 h post-transfection. Results shown are from a representative experiment performed in triplicate. *E*, viability of HEK293A cells was assessed in parallel with data shown in *panel D*. *F*, HEK293A cells were transiently co-transfected with pGL3-ASAH1 and pIRES-GFP or pCerS6-IRES-GFP in the absence and presence of 100 μM FB1 or with mutant CerS6 (H212A). Luciferase activity was determined 28 h post-transfection. Results shown are the mean fold-increase ± S.E. from two independent experiments. *, $p < 0.05$; ***, $p < 0.0005$.

LCL-521 (26). As shown in Fig. 5*C*, HT-CerS6 cells were more susceptible to inhibition of acid ceramidase than HT-GFP cells.

Transcriptional Activation of Acid Ceramidase by Ceramide Synthases—The increase in acid ceramidase (ASAH1) mRNA suggested that CerS6 may transcriptionally activate expression of this enzyme. To further explore this possibility, we stably transfected HT29 cells with pGL3-ASAH1, a plasmid in which luciferase expression is under control of the full-length acid ceramidase promoter (23). Stable transfectants were then transduced with an adenovirus-expressing CerS6 (AdCerS6). As shown in Fig. 6*A*, the control virus did not alter ASAH1-driven luciferase activity whereas AdCerS6 increased luminescence 2–3-fold. Next, we asked whether the ability to transcriptionally activate acid ceramidase expression is unique to CerS6. HEK293A cells were co-transfected with the acid ceramidase reporter construct (pGL3-ASAH1) and plasmids expressing CerS1–6. Expression of CerS3–6 transcriptionally activated the ASAH1 promoter as evidenced by a significant ~2-fold increase in luciferase reporter gene activity (Fig. 6*B*). Expression of CerS1 did not significantly alter ASAH1 reporter activity while expression of CerS2 slightly but significantly decreased luciferase activity.

Since treatment with SP600125 or curcumin decreased acid ceramidase expression in HT-CerS6 cells, we next investigated how these inhibitors affect transcriptional activation of ASAH1. We verified based on GFP expression that neither inhibitor interfered with transfection efficiency. When CerS6 was expressed in the presence of SP600125, ASAH1 reporter activity was not significantly different from GFP-transfected cells (Fig. 6*C*). We found that similar to inhibition of JNK, treatment with 25 μM curcumin prevented the CerS6-mediated transcriptional activation of acid ceramidase (Fig. 6*C*).

Next, we investigated whether the increase in ASAH1 transcription upon elevated CerS6 expression is a direct consequence of increased generation of C_{16}-ceramide. HEK293A cells were transfected with pGL3-ASAH1 and after 20 h, C_{16}-ceramide was exogenously added for 6 h. In the presence of 10 μM C_{16}-ceramide we did not observe an increase in pGL3-ASAH1 reporter activity (Fig. 6*D*). At higher concentrations of exogenous C_{16}-ceramide luciferase reporter activity declined, and cells began to lose viability (Fig. 6, *D* and *E*). Similarly exogenous C_6-ceramide, which is preferentially metabolized into C_{16}-ceramide but was less toxic under our assay conditions failed to alter luciferase reporter gene activity (Fig. 6, *D* and *E*). Furthermore, the ceramide synthase inhibitor fumonison B1 did not prevent the CerS6-induced increase luciferase reporter activity, suggesting that enzymatic activity does not significantly contribute to increased acid ceramidase expression (Fig. 6*F*). Finally, to substantiate this observation, we utilized a CerS6 mutant in which the catalytic domain has been inactivated through a histone to alanine substitution at residue 212 (15). As shown in Fig. 6*F*, mutant H212A CerS6 retained the ability to significantly increase pGL3-ASAH1 reporter activity.

Discussion

Several groups including ours have shown that decreased expression of CerS6 results in a specific decrease in C_{16}-ceramide (3, 37). The current study was initiated to understand how overexpression of CerS6 impacts on sphingolipid composition and signaling. We show that cells with increased expression of CerS6 preferentially generate C_{16}-ceramide, which is consistent with previously observed activity of the enzyme *in vitro* (1). Incorporation of sphingosine into ceramide was comparable between HT-GFP and HT-CerS6 cells, suggesting that the increase in C_{16}-ceramide occurred at the expense of saturated very long chain ceramides ($C_{22:0}$, $C_{24:0}$, and $C_{26:0}$) (Fig. 2). Similar results have been observed in models that modulate other CerS family members. For example, in CerS2-deficient mice and in SMS-KCNR neuroblastoma cells treated with CerS2 RNAi, long chain ceramides such as C_{16}-Cer compensated for the decrease in C_{24}- and $C_{24:1}$- ceramides (13, 38). Mullen *et al.* also showed that down-regulation of individual CerS in MCF7 breast cancer cells can transcriptionally impact the expression of non-targeted CerS (37). The distribution of ceramide species was mirrored in sphingomyelin composition (Fig. 3), suggesting that incorporation of ceramides into complex sphingolipids occurs without preference for a specific ceramide species.

In addition to altered ceramide composition, HT29 cells expressing CerS6 also contained increased intracellular sphingosine, which suggested the possibility that CerS6 expression also increases ceramidase expression and activity. Our results indicate that expression of CerS6 can stimulate expression of acid ceramidase, resulting in increased mRNA, protein expression and activity of the enzyme (Fig. 4, *A*–*C*). The increase in acid ceramidase following CerS6 expression was not unique to HT29 cells and was also observed in SW620 colon cancer cells that overexpress CerS6 (previously described in (3)) as well as in PPC1 prostate cancer cells transduced with an adenovirus expressing CerS6 (34). These data suggest that the increase in acid ceramidase following CerS6 expression is not a cell line or tissue-specific response.

Interestingly, both HT29 and SW620 cells transfected with CerS6 express higher levels of acid ceramidase, yet are more susceptible to apoptotic stimuli (3, 6). This is in contrast to prostate cancer cells in which elevated acid ceramidase expression has been associated with apoptosis resistance and relapse following radiation therapy (34, 39). It was previously observed that an increase in acid ceramidase, which is a lysosomal enzyme, resulted in elevated lysosomal density and increased levels of autophagy (40). Autophagy has been demonstrated to serve as a cellular mechanism to limit ceramide levels in the liver (41) and also occurs as a consequence of increased sphingolipid synthesis in RAW264.7 cells following TLR4 stimulation (42). In contrast to these studies, we did not detect an increase in overall ceramide synthesis but rather a shift in composition (Fig. 2) and using lysotracker staining we were unable to detect any differences in lysosomal density.[4] One possibility for the discrepancy in apoptotic responsiveness between prostate cancer cells and our model system are differences in subsequent metabolism of sphingosine that is generated as a consequence of increased acid ceramidase expression. Sphingosine holds a unique position in sphingolipid metabolism in that it can be further metabolized to sphingosine-1-phosphate (S1P) by sphingosine kinases or serve as a substrate for ceramide synthases in the salvage pathway (10). Irradiation of prostate cancer cells increased the pro-apoptotic sphingolipids ceramide and sphingosine but also elevated sphingosine-1-phosphate (S1P), indicating that sphingosine was further metabolized by sphingosine kinases (34). In contrast, in HT29 colon cancer cells intracellular S1P generation is greatly diminished upon CerS6 expression (Fig. 4*E*). It is possible that ceramide synthases and sphingosine kinases compete for the sphingosine substrate, although this idea would need to be reconciled with subcellular localization of the enzymes involved. Ceramide synthases are primarily localized to the ER and have also been detected in mitochondria, while sphingosine kinases have been localized to cytosol/plasma membrane (SK1) or the nucleus (SK2) (43). Therefore, although sphingosine is a soluble product of sphingolipid metabolism, it is unlikely that ceramide synthases and sphingosine kinases directly compete for the substrate in the same compartment. While details remain to be investigated, the increased apoptotic susceptibility of HT-CerS6 or SW620-CerS6 cells, despite elevated acid ceramidase expression, may offer an explanation for recent studies in ovarian and

[4] C. Voelkel-Johnson, unpublished data.

breast cancers where elevated expression of acid ceramidase correlated with a better prognosis (44, 45).

We also observed that HT-CerS6 cells were more susceptible to treatment with the acid ceramidase inhibitor LCL-521 (Fig. 5*C*), which suggests higher levels of acid ceramidase maybe important for cells to maintain viability when CerS6 expression is elevated. However, as a consequence of elevated acid ceramidase activity, intracellular levels of sphingosine increase, which may result in heightened susceptibility to apoptotic signals either in a therapeutic setting or endogenously through the immune system. The dynamic nature of sphingolipids and the complexity of crosstalk between sphingolipid metabolic pathways, suggests it may be very difficult to utilize a single sphingolipid enzyme such as acid ceramidase as a biomarker for prognosis or therapy responsiveness.

Using an ASAH1-promoter driven luciferase reporter plasmid, we confirmed that CerS6 induced transcriptional up-regulation of acid ceramidase (Fig. 6). Experiments with pharmacological inhibitors suggest that transcriptional activation of acid ceramidase by CerS6 occurs in a JNK/AP-1-dependent manner (Figs. 5 and 6). These results are consistent with previous studies that show activation of the JNK pathway following ceramide stress as well as with ceramide/AP-1-dependent transcriptional activation of acid ceramidase following radiation therapy in prostate cancer cells (31–34). JNK belongs to the larger group of mitogen-activated protein kinases and responds to a variety of signals including cytokines, radiation, heat shock, and autophagy (46, 47). How CerS6 overexpression impacts on signaling pathways other than apoptosis largely remains to be determined.

Curcumin, which also inhibited CerS6-induced transcriptional induction of acid ceramidase, affects numerous signaling pathways. In addition to inhibiting AP-1 binding, it has recently been shown to stimulate ceramide synthase activity through increased CerS dimer formation (48). Although it is unclear whether CerS dimer formation can occur at the concentration of curcumin used in our study (25 μM *versus* 50 μM), these studies suggest an impact of curcumin on sphingolipid signaling may possibly occur through both down-regulation of acid ceramidase expression and increased CerS dimer formation.

To investigate if the ability to enhance acid ceramidase transcription is unique to CerS6, we extended our study to all members of the CerS family. CerS1 was the only CerS family member that did not alter acid ceramidase reporter activity, which was not completely unexpected, as CerS1 is phylogenetically the most distant family member and appears to have functions that are distinct from CerS6 (49). For example, CerS1 but not CerS6 has been shown to induce mitophagy (50). Transfection of the CerS2 plasmid slightly but significantly decreased ASAH1-promoter-driven reporter activity (Fig. 6*B*). Whether the opposing effects of CerS2 and CerS6 on transcriptional activation of acid ceramidase is a consequence of differential heterodimer composition remains to be investigated. CerS3, -4, and -5 shared the capacity of CerS6 to stimulate transcriptional activation of acid ceramidase. Somewhat surprisingly, there was no correlation between the ability to stimulate ASAH1-luc reporter activity and the fatty acid specificities of the CerS isoforms (19). For example, both CerS1 and CerS4 can generate C_{18}-ceramide, yet transcriptional activation of ASAH1-luc was only observed with CerS4 and not CerS1. A similar discrepancy was observed between CerS2 and CerS3/4, which have overlapping abilities to generate very long chain ceramides (19).

To further investigate the requirement for ceramide synthase activity for induction of acid ceramidase transcription, we used three different approaches: exogenously added ceramide, the CerS inhibitor FB1, and a CerS6 mutant that lacks catalytic activity. Exogenous ceramide failed to induce ASAH1-luc reporter activity, while FB1 and the CerS6 H212A mutant failed to significantly reduce it. Taken together, these results suggest that transcriptional activation of acid ceramidase in our model is not mediated by ceramide itself and does not depend on the catalytic activity of CerS. Recently it has been demonstrated that ectopically expressed Bcl2L13 binds to CerS6 (51). Therefore, one possibility is that elevated expression of acid ceramidase in response to CerS6 overexpression occurs as a consequence of altered protein-protein interactions with non-CerS proteins. This hypothesis would also explain why knockdown of CerS6 did not decrease acid ceramidase expression in SW480 cells (Fig. 4*F*). Future studies to investigate CerS binding partners may elucidate the exact mechanism by which overexpression of CerS6 (or CerS3, 4, 5) mediates a transcriptional increase in acid ceramidase.

Conclusions

This study shows how altered expression of a single ceramide synthase has profound effects on the sphingolipid network, impacting both sphingolipid composition as well as acid ceramidase expression, which leads to alterations in signaling pathways and cell death susceptibility.

Furthermore, our results suggest that the catalytic activity of CerS6 is not required for the ability to transcriptionally activate acid ceramidase expression, thereby revealing a new level of complexity by which ceramide synthases can impact cellular responses.

Acknowledgments—We thank Dr. Marion Sewer for the pGL3-ASAH1 reporter plasmid, Dr. Tony Futerman for the CerS expression plasmids, and members of the Hollings Cancer Center Lipids in Cancer Signaling group for helpful discussions of this project.

References

1. Mullen, T. D., Hannun, Y. A., and Obeid, L. M. (2012) Ceramide synthases at the centre of sphingolipid metabolism and biology. *Biochem. J.* **441,** 789–802
2. Grösch, S., Schiffmann, S., and Geisslinger, G. (2012) Chain length-specific properties of ceramides. *Prog. Lipid Res.* **51,** 50–62
3. White-Gilbertson, S., Mullen, T., Senkal, C., Lu, P., Ogretmen, B., Obeid, L., and Voelkel-Johnson, C. (2009) Ceramide synthase 6 modulates TRAIL sensitivity and nuclear translocation of active caspase-3 in colon cancer cells. *Oncogene* **28,** 1132–1141
4. Walker, T., Mitchell, C., Park, M. A., Yacoub, A., Rahmani, M., Häussinger, D., Reinehr, R., Voelkel-Johnson, C., Fisher, P. B., Grant, S., and Dent, P. (2010) 17-allylamino-17-demethoxygeldanamycin and MEK1/2 inhibitors kill GI tumor cells via Ca2+-dependent suppression of GRP78/BiP and induction of ceramide and reactive oxygen species. *Mol Cancer Ther* **9,** 1378–1395
5. Park, M. A., Walker, T., Martin, A. P., Allegood, J., Vozhilla, N., Emdad, L., Sarkar, D., Rahmani, M., Graf, M., Yacoub, A., Koumenis, C., Spiegel, S.,

Curiel, D. T., Voelkel-Johnson, C., Grant, S., Fisher, P. B., and Dent, P. (2009) MDA-7/IL-24-induced cell killing in malignant renal carcinoma cells occurs by a ceramide/CD95/PERK-dependent mechanism. *Mol. Cancer Ther.* **8,** 1280–1291
6. Walker, T., Mitchell, C., Park, M. A., Yacoub, A., Graf, M., Rahmani, M., Houghton, P. J., Voelkel-Johnson, C., Grant, S., and Dent, P. (2009) Sorafenib and vorinostat kill colon cancer cells by CD95-dependent and -independent mechanisms. *Mol. Pharmacol.* **76,** 342–355
7. Park, M. A., Mitchell, C., Zhang, G., Yacoub, A., Allegood, J., Häussinger, D., Reinehr, R., Larner, A., Spiegel, S., Fisher, P. B., Voelkel-Johnson, C., Ogretmen, B., Grant, S., and Dent, P. (2010) Vorinostat and sorafenib increase CD95 activation in gastrointestinal tumor cells through a Ca(2+)-de novo ceramide-PP2A-reactive oxygen species-dependent signaling pathway. *Cancer Res.* **70,** 6313–6324
8. Schiffmann, S., Ziebell, S., Sandner, J., Birod, K., Deckmann, K., Hartmann, D., Rode, S., Schmidt, H., Angioni, C., Geisslinger, G., and Grösch, S. (2010) Activation of ceramide synthase 6 by celecoxib leads to a selective induction of C16:0-ceramide. *Biochem. Pharmacol.* **80,** 1632–1640
9. Separovic, D., Breen, P., Joseph, N., Bielawski, J., Pierce, J. S., Van Buren, E., and Gudz, T. I. (2012) Ceramide synthase 6 knockdown suppresses apoptosis after photodynamic therapy in human head and neck squamous carcinoma cells. *Anticancer Res.* **32,** 753–760
10. Tirodkar, T. S., and Voelkel-Johnson, C. (2012) Sphingolipids in apoptosis. *Exp. Oncol.* **34,** 231–242
11. Hartmann, D., Lucks, J., Fuchs, S., Schiffmann, S., Schreiber, Y., Ferreiros, N., Merkens, J., Marschalek, R., Geisslinger, G., and Grosch, S. Long chain ceramides and very long chain ceramides have opposite effects on human breast and colon cancer cell growth. *Int. J. Biochem. Cell Biol.* **44,** 620–628
12. Mesicek, J., Lee, H., Feldman, T., Jiang, X., Skobeleva, A., Berdyshev, E. V., Haimovitz-Friedman, A., Fuks, Z., and Kolesnick, R. (2010) Ceramide synthases 2, 5, and 6 confer distinct roles in radiation-induced apoptosis in HeLa cells. *Cell Signal.* **22,** 1300–1307
13. Pewzner-Jung, Y., Park, H., Laviad, E. L., Silva, L. C., Lahiri, S., Stiban, J., Erez-Roman, R., Brügger, B., Sachsenheimer, T., Wieland, F., Prieto, M., Merrill, A. H., Jr., and Futerman, A. H. (2010) A critical role for ceramide synthase 2 in liver homeostasis: I. alterations in lipid metabolic pathways. *J. Biol. Chem.* **285,** 10902–10910
14. Pewzner-Jung, Y., Brenner, O., Braun, S., Laviad, E. L., Ben-Dor, S., Feldmesser, E., Horn-Saban, S., Amann-Zalcenstein, D., Raanan, C., Berkutzki, T., Erez-Roman, R., Ben-David, O., Levy, M., Holzman, D., Park, H., Nyska, A., Merrill, A. H., Jr., and Futerman, A. H. (2010) A critical role for ceramide synthase 2 in liver homeostasis: II. insights into molecular changes leading to hepatopathy. *J. Biol. Chem.* **285,** 10911–10923
15. Senkal, C. E., Ponnusamy, S., Bielawski, J., Hannun, Y. A., and Ogretmen, B. (2010) Antiapoptotic roles of ceramide-synthase-6-generated C16-ceramide via selective regulation of the ATF6/CHOP arm of ER-stress-response pathways. *FASEB J.* **24,** 296–308
16. Senkal, C. E., Ponnusamy, S., Manevich, Y., Meyers-Needham, M., Saddoughi, S. A., Mukhopadyay, A., Dent, P., Bielawski, J., and Ogretmen, B. (2011) Alteration of ceramide synthase 6/C16-ceramide induces activating transcription factor 6-mediated endoplasmic reticulum (ER) stress and apoptosis via perturbation of cellular Ca2+ and ER/Golgi membrane network. *J. Biol. Chem.* **286,** 42446–42458
17. Park, J. W., Park, W. J., and Futerman, A. H. (2014) Ceramide synthases as potential targets for therapeutic intervention in human diseases. *Biochim. Biophys. Acta* **1841,** 671–681
18. Schiffmann, S., Ferreiros, N., Birod, K., Eberle, M., Schreiber, Y., Pfeilschifter, W., Ziemann, U., Pierre, S., Scholich, K., Grösch, S., and Geisslinger, G. (2012) Ceramide synthase 6 plays a critical role in the development of experimental autoimmune encephalomyelitis. *J. Immunol.* **188,** 5723–5733
19. Levy, M., and Futerman, A. H. (2010) Mammalian ceramide synthases. *IUBMB life* **62,** 347–356
20. Coetzee, T., Fujita, N., Dupree, J., Shi, R., Blight, A., Suzuki, K., and Popko, B. (1996) Myelination in the absence of galactocerebroside and sulfatide: normal structure with abnormal function and regional instability. *Cell* **86,** 209–219
21. Meixner, M., Jungnickel, J., Grothe, C., Gieselmann, V., and Eckhardt, M. (2011) Myelination in the absence of UDP-galactose:ceramide galactosyltransferase and fatty acid 2 -hydroxylase. *BMC Neurosci.* **12,** 22
22. Lahiri, S., Lee, H., Mesicek, J., Fuks, Z., Haimovitz-Friedman, A., Kolesnick, R. N., and Futerman, A. H. (2007) Kinetic characterization of mammalian ceramide synthases: determination of K(m) values towards sphinganine. *FEBS Letters* **581,** 5289–5294
23. Lucki, N., and Sewer, M. B. (2009) The cAMP-responsive element binding protein (CREB) regulates the expression of acid ceramidase (ASAH1) in H295R human adrenocortical cells. *Biochim. Biophys. Acta* **1791,** 706–713
24. Wiederschain, D., Wee, S., Chen, L., Loo, A., Yang, G., Huang, A., Chen, Y., Caponigro, G., Yao, Y. M., Lengauer, C., Sellers, W. R., and Benson, J. D. (2009) Single-vector inducible lentiviral RNAi system for oncology target validation. *Cell Cycle* **8,** 498–504
25. Luo, J., Deng, Z. L., Luo, X., Tang, N., Song, W. X., Chen, J., Sharff, K. A., Luu, H. H., Haydon, R. C., Kinzler, K. W., Vogelstein, B., and He, T. C. (2007) A protocol for rapid generation of recombinant adenoviruses using the AdEasy system. *Nat. Protoc* **2,** 1236–1247
26. Bai, A., Szulc, Z. M., Bielawski, J., Pierce, J. S., Rembiesa, B., Terzieva, S., Mao, C., Xu, R., Wu, B., Clarke, C. J., Newcomb, B., Liu, X., Norris, J., Hannun, Y. A., and Bielawska, A. (2014) Targeting (cellular) lysosomal acid ceramidase by B13: Design, synthesis and evaluation of novel DMG-B13 ester prodrugs. *Bioorgan. Med. Chem.* **22,** 6933–6944
27. Voelkel-Johnson, C., Hannun, Y. A., and El-Zawahry, A. (2005) Resistance to TRAIL is associated with defects in ceramide signaling that can be overcome by exogenous C6-ceramide without requiring down-regulation of cellular FLICE inhibitory protein. *Mol. Cancer Ther.* **4,** 1320–1327
28. Bielawski, J., Pierce, J. S., Snider, J., Rembiesa, B., Szulc, Z. M., and Bielawska, A. (2010) Sphingolipid analysis by high performance liquid chromatography-tandem mass spectrometry (HPLC-MS/MS). *Adv. Exp. Med. Biol.* **688,** 46–59
29. Van Veldhoven, P. P., and Bell, R. M. (1988) Effect of harvesting methods, growth conditions and growth phase on diacylglycerol levels in cultured human adherent cells. *Biochim. Biophys. Acta* **959,** 185–196
30. Spassieva, S., Bielawski, J., Anelli, V., and Obeid, L. M. (2007) Combination of C(17) sphingoid base homologues and mass spectrometry analysis as a new approach to study sphingolipid metabolism. *Methods Enzymol.* **434,** 233–241
31. Ruvolo, P. P. (2003) Intracellular signal transduction pathways activated by ceramide and its metabolites. *Pharmacol. Res.* **47,** 383–392
32. Verheij, M., Bose, R., Lin, X. H., Yao, B., Jarvis, W. D., Grant, S., Birrer, M. J., Szabo, E., Zon, L. I., Kyriakis, J. M., Haimovitz-Friedman, A., Fuks, Z., and Kolesnick, R. N. (1996) Requirement for ceramide-initiated SAPK/JNK signalling in stress-induced apoptosis. *Nature* **380,** 75–79
33. Westwick, J. K., Bielawska, A. E., Dbaibo, G., Hannun, Y. A., and Brenner, D. A. (1995) Ceramide activates the stress-activated protein kinases. *J. Biol. Chem.* **270,** 22689–22692
34. Cheng, J. C., Bai, A., Beckham, T. H., Marrison, S. T., Yount, C. L., Young, K., Lu, P., Bartlett, A. M., Wu, B. X., Keane, B. J., Armeson, K. E., Marshall, D. T., Keane, T. E., Smith, M. T., Jones, E. E., Drake, R. R., Jr., Bielawska, A., Norris, J. S., and Liu, X. (2013) Radiation-induced acid ceramidase confers prostate cancer resistance and tumor relapse. *J. Clin. Investig.* **123,** 4344–4358
35. Bierhaus, A., Zhang, Y., Quehenberger, P., Luther, T., Haase, M., Müller, M., Mackman, N., Ziegler, R., and Nawroth, P. P. (1997) The dietary pigment curcumin reduces endothelial tissue factor gene expression by inhibiting binding of AP-1 to the DNA and activation of NF-κB. *Thrombosis Haemostasis* **77,** 772–782
36. Huang, T. S., Lee, S. C., and Lin, J. K. (1991) Suppression of c-Jun/AP-1 activation by an inhibitor of tumor promotion in mouse fibroblast cells. *Proc. Natl. Acad. Sci. U. S. A.* **88,** 5292–5296
37. Mullen, T. D., Spassieva, S., Jenkins, R. W., Kitatani, K., Bielawski, J., Hannun, Y. A., and Obeid, L. M. (2011) Selective knockdown of ceramide synthases reveals complex interregulation of sphingolipid metabolism. *J. Lipid Res.* **52,** 68–77
38. Spassieva, S. D., Mullen, T. D., Townsend, D. M., and Obeid, L. M. (2009) Disruption of ceramide synthesis by CerS2 down-regulation leads to autophagy and the unfolded protein response. *Biochem. J.* **424,** 273–283

39. Seelan, R. S., Qian, C., Yokomizo, A., Bostwick, D. G., Smith, D. I., and Liu, W. (2000) Human acid ceramidase is overexpressed but not mutated in prostate cancer. *Genes Chromosomes Cancer* **29,** 137–146
40. Turner, L. S., Cheng, J. C., Beckham, T. H., Keane, T. E., Norris, J. S., and Liu, X. (2011) Autophagy is increased in prostate cancer cells overexpressing acid ceramidase and enhances resistance to C6 ceramide. *Prostate Cancer and Prostatic Diseases* **14,** 30–37
41. Alexaki, A., Gupta, S. D., Majumder, S., Kono, M., Tuymetova, G., Harmon, J. M., Dunn, T. M., and Proia, R. L. (2014) Autophagy regulates sphingolipid levels in the liver. *J. Lipid Res.* **55,** 2521–2531
42. Sims, K., Haynes, C. A., Kelly, S., Allegood, J. C., Wang, E., Momin, A., Leipelt, M., Reichart, D., Glass, C. K., Sullards, M. C., and Merrill, A. H., Jr. (2010) Kdo2-lipid A, a TLR4-specific agonist, induces de novo sphingolipid biosynthesis in RAW264.7 macrophages, which is essential for induction of autophagy. *J. Biol. Chem.* **285,** 38568–38579
43. Gault, C. R., Obeid, L. M., and Hannun, Y. A. (2010) An overview of sphingolipid metabolism: from synthesis to breakdown. *Adv. Exp. Med. Biol.* **688,** 1–23
44. Sänger, N., Ruckhäberle, E., Györffy, B., Engels, K., Heinrich, T., Fehm, T., Graf, A., Holtrich, U., Becker, S., and Karn, T. (2015) Acid ceramidase is associated with an improved prognosis in both DCIS and invasive breast cancer. *Mol. Oncol.* **9,** 58–67
45. Hanker, L. C., Karn, T., Holtrich, U., Gätje, R., Rody, A., Heinrich, T., Ruckhäberle, E., and Engels, K. (2013) Acid ceramidase (AC)–a key enzyme of sphingolipid metabolism– correlates with better prognosis in epithelial ovarian cancer. *Int. J. Gynecol. Pathol.* **32,** 249–257
46. Sehgal, V., and Ram, P. T. (2013) Network Motifs in JNK Signaling. *Genes Cancer* **4,** 409–413
47. Tang, H. W., Liao, H. M., Peng, W. H., Lin, H. R., Chen, C. H., and Chen, G. C. (2013) Atg9 interacts with dTRAF2/TRAF6 to regulate oxidative stress-induced JNK activation and autophagy induction. *Dev. Cell* **27,** 489–503
48. Laviad, E. L., Kelly, S., Merrill, A. H., Jr., and Futerman, A. H. (2012) Modulation of ceramide synthase activity via dimerization. *J. Biol. Chem.* **287,** 21025–21033
49. Pewzner-Jung, Y., Ben-Dor, S., and Futerman, A. H. (2006) When do Lasses (longevity assurance genes) become CerS (ceramide synthases)?: Insights into the regulation of ceramide synthesis. *J. Biol. Chem.* **281,** 25001–25005
50. Sentelle, R. D., Senkal, C. E., Jiang, W., Ponnusamy, S., Gencer, S., Selvam, S. P., Ramshesh, V. K., Peterson, Y. K., Lemasters, J. J., Szulc, Z. M., Bielawski, J., and Ogretmen, B. (2012) Ceramide targets autophagosomes to mitochondria and induces lethal mitophagy. *Nature Chemical Biology* **8,** 831–838
51. Jensen, S. A., Calvert, A. E., Volpert, G., Kouri, F. M., Hurley, L. A., Luciano, J. P., Wu, Y., Chalastanis, A., Futerman, A. H., and Stegh, A. H. (2014) Bcl2L13 is a ceramide synthase inhibitor in glioblastoma. *Proc. Natl. Acad. Sci. U. S. A.* **111,** 5682–5687